Direct Resistance Comparisons From the QHR to 100 MΩ Using a Cryogenic Current Comparator

Randolph E. Elmquist, *Senior Member, IEEE*, Emmanouel Hourdakis, Dean G. Jarrett, *Senior Member, IEEE*, and Neil M. Zimmerman

***Abstract*—Measurements of room-temperature 100 MΩ standard resistors and cryogenic thin-film resistors based directly on a quantized Hall resistance standard have been made with a cryogenic current comparator (CCC) bridge. This 15 496:2 ratio CCC attains a current sensitivity of 10.7 $\mathrm{fA/Hz^{1/2}}$ in measurements of cryogenic thin-film resistors, without extensive shielding or filtering. A resistive primary winding helps the CCC maintain stability in the presence of external noise. The resistive-winding technique may be useful for the absolute measurement of small currents delivered by single-electron tunneling devices.**

***Index Terms*—Johnson noise, quantum Hall effect, resistance standards, single-electron tunneling.**

I. Introduction

SOME of the earliest cryogenic current comparator (CCC) bridges used superconducting windings and interconnections to determine a ratio of two-terminal resistances [1], [2]. In these bridges identical voltages appear across the resistors to be compared, and the two-terminal resistance ratio can be calculated solely from the ampere-turns balance detected and maintained by a superconducting quantum interference device (SQUID). While these bridges were developed to compare cryogenic resistors, with slight modifications the design can be applied to other classes of resistor including the quantized Hall resistance (QHR) and high-value resistance standards. This paper describes such a two-terminal CCC technique based on comparing a 100 MΩ resistor directly with the QHR. One additional goal of this work is to improve the performance of CCC-based current detectors in order to measure absolute currents from single-electron tunneling (SET) devices in the quantum units of the SI volt and the SI ohm. In [3], Elmquist *et al.* describe a CCC method of balancing the SET current against a current generated by a calibrated thin-film, cryogenic 100 MΩ resistor and a Josephson device.

In the resistance scaling process used today to maintain many national representations of the SI ohm, four-terminal standard resistors are compared to the QHR standard using CCC bridges. These CCC measurements generally transfer SI values to resistors near 100 Ω. Two isolated windings and a SQUID detect the current ratio while a sensitive voltage detector measures the difference in potential across the standards. In contrast, the two-terminal CCC is similar in concept to bridges such as the active-arm bridge [4] and the Josephson potentiometer [5].

Manuscript received July 2, 2004; revised September 30, 2004.

The authors are with the National Institute of Standards and Technology, Gaithersburg, MD 20899-8171 USA.

Digital Object Identifier 10.1109/TIM.2004.843330

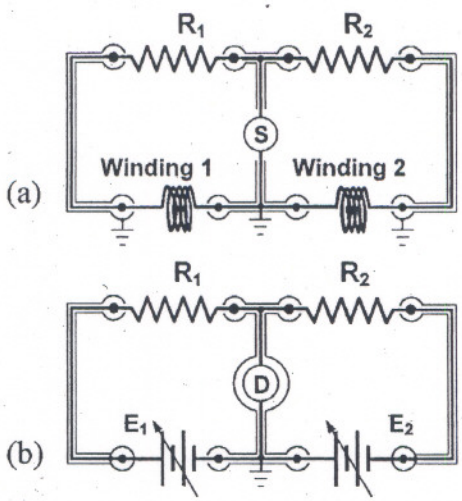

Fig. 1. (a) Schematic diagram of the two-terminal CCC bridge with two detection windings, where R_1 is the unknown, R_2 is the standard, and S is a voltage or current source. (b) Schematic diagram of the active-arm high-resistance bridge, where E_1 and E_2 are adjustable voltage sources and D is a voltage or current detector.

Fig. 1(a) shows a schematic diagram of a two-terminal CCC bridge. When the functions of detectors and sources are exchanged, as in Fig. 1(b), a working active-arm bridge is the result. This duality is observed in many types of impedance bridges.

II. Design Considerations

As pictured in Fig. 2, the Delahaye scheme of multiple connections [6] should be used when a QHR standard is used for two-terminal measurements. A set of three leads is connected to device contacts at the measurement potential and a second set is connected to contacts close to ground potential. These six leads from the quantum Hall effect (QHE) device are brought out of the cryostat. The sets of leads are then connected together inside a separate CCC cryostat at two superconducting junctions. In a device with near zero longitudinal resistance, this ensures that negligible current flows through the two central transverse QHE terminals.

The CCC winding N_2 on the QHR side of the bridge is also superconducting, making the voltage across the QHE device identical to that across the primary bridge arm except for small thermal voltages. As with the four-terminal CCC, the slowly changing thermal voltages are largely eliminated by reversing the excitation current periodically. The excitation current should be ramped to zero when it is reversed to ensure that the SQUID feedback (supplied through a sense resistor, R_3) maintains flux

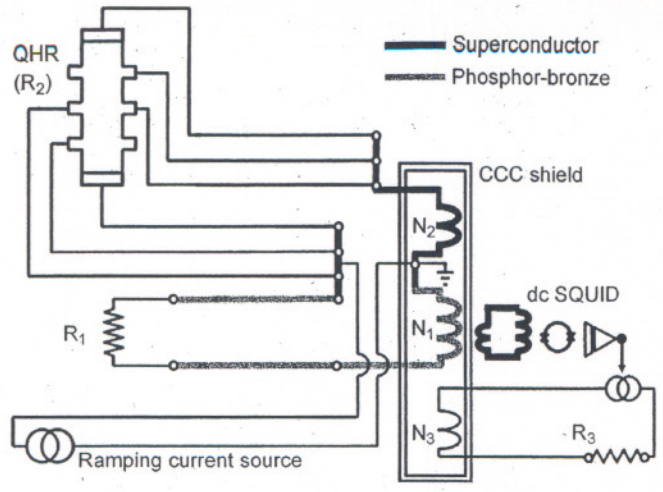

Fig. 2. Design of a CCC bridge for comparisons between the QHR standard and a 100 MΩ resistor (R_1). The feedback current I_3 is determined by measuring the voltage across resistor R_3.

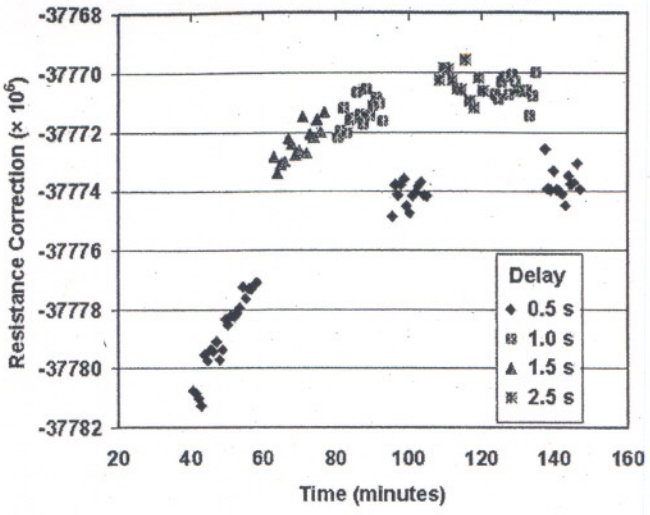

Fig. 3. Graph of a sequence of CCC ratio data for a cryogenic resistance sample of value near 96.2 MΩ with source current $I_0 = 73\ \mu$A. The time given in the inset is a variable delay in the measurement sequence that allows for settling of bridge currents, as explained in the text.

lock throughout the measurement. Transient signals from the single source are largely cancelled in the two-terminal bridge by the opposing CCC windings if the resistance ratio is close to the winding ratio. While no voltage detector is required in this two-terminal bridge, the essential similarity between the two types of CCC bridges is that the voltage applied to the two standards must be nearly equal, and may be limited by the quantization breakdown current of the QHE device.

The major differences between the two types of bridge are that 1) when the leads and winding in the primary arm of the two-terminal bridge are not superconducting, it is necessary to independently measure and correct for their resistance. Specifically, the resistance of leads and windings must be subtracted from the measurement result to find the value of the primary resistor. 2) The noise level for the two-terminal CCC is limited only by the Johnson noise current of the high-value resistor and the SQUID noise, since there is no voltage detector, and 3) the two-terminal bridge excitation level in ampere-turns is small because the QHR is used in the secondary bridge arm, which utilizes of order 10 turns.

The two-terminal CCC bridge balance equations are

$$I_1 R_1 = I_2 R_2 \tag{1}$$

and

$$I_1 N_1 = I_2 N_2 + \delta \tag{2}$$

where currents I_1 and I_2 flow through resistances R_1 and R_2, respectively, and δ is the ampere-turns imbalance for windings N_1 and N_2. If a third, isolated CCC winding N_3 is supplied with a balancing feedback current derived from the SQUID, this second equation can be written as

$$I_1 N_1 = I_2 N_2 + I_3 N_3. \tag{3}$$

These equations yield

$$R_1 = R_2 \left(\frac{N_1}{N_2}\right)\left(1 - \frac{I_3 N_3}{I_1 N_1}\right). \tag{4}$$

The total current is $I_0 = I_1 + I_2$. Since the voltages across R_1 and R_2 are identical

$$I_1 = I_0 \left(\frac{R_2}{R_1 + R_2}\right). \tag{5}$$

The first four equations above also apply to those four-terminal CCC bridges that use voltage-balancing feedback.

III. Cryogenic 100 MΩ Resistors

Chromium thin-film resistors were prepared using photolithography and electron-beam deposition. One 96.2 MΩ resistor was used in the bridge to test both the bridge settling time and the noise performance with the resistor at 4.2 K. CCC tests on these resistors have shown that the barometric pressure in the laboratory has a noticeable effect on the resistance, through its effect on the temperature of the liquid helium bath. The bridge equations also show that any drift in I_0 will contribute to drift in I_3. This effect is more noticeable when R_1 is far from its nominal value of 100 MΩ and I_3 is large. These factors are a source of long-term instability but are not considered to be significant sources of short-term noise.

The current I_0 is produced from an isolated, battery-powered, digitally-ramped voltage source together with a voltage-to-current source. The current reversal ramp-time can be set between 1.25 s and 9.0 s. At the current reversal, if the required change in the feedback current I_3 is small, the SQUID output level remains within about $10^{-3}\ \Phi_0$ (1 mV) of zero for room-temperature standard resistors with values very close to 100 MΩ. Here, Φ_0 indicates a SQUID excitation of one magnetic flux quantum.

Fig. 3 shows CCC ratio data for the cryogenic resistor where the feedback current I_3 supplied about 3.8% of the total CCC signal, causing a transient SQUID deflection of about 0.1 Φ_0 (100 mV) at the current reversal. The abrupt shifts in the ratio seen in Fig. 3 were caused by deliberate changes in the settling time delay used in the measurement sequence after each reversal of the current I_0. A variable settling time t between 0.5 s and

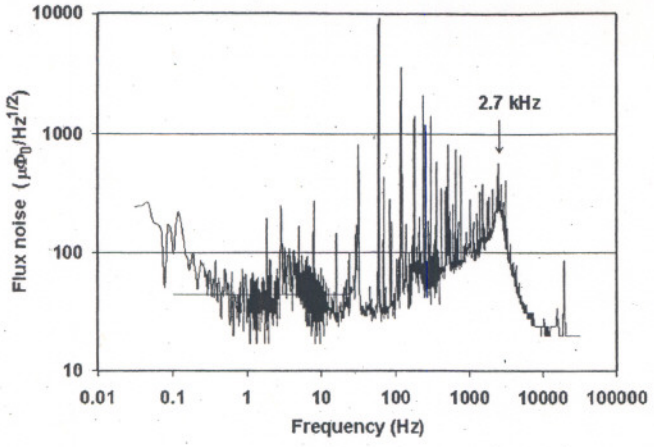

Fig. 4. SQUID flux noise spectrum for the resistive-winding CCC in a comparison of the QHR with a 96.2 MΩ chromium resistance sample. A straight line is drawn at 44 $\mu\Phi_0/\mathrm{Hz}^{1/2}$, showing the weighted average flux noise between 0.1 Hz and 25 Hz. The SQUID sensitivity falls off inversely with frequency above about 1 kHz.

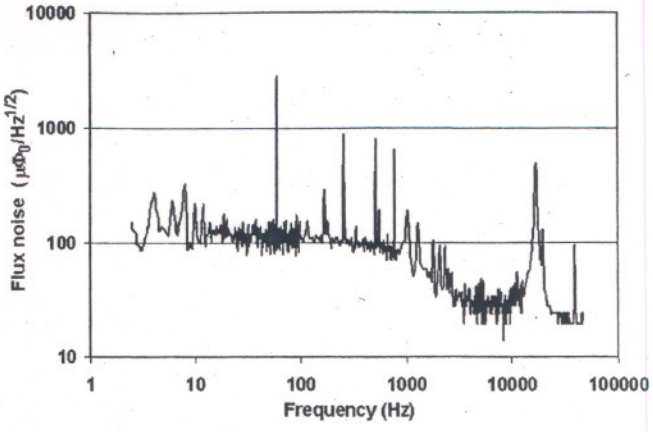

Fig. 5. SQUID flux noise spectrum for a superconducting-winding CCC in a comparison QHR with a 1 MΩ room-temperature standard resistor. The noise resonance occurs at 20 kHz, and the SQUID sensitivity falls off inversely with frequency above about 1 kHz.

2.5 s was used at the end of the 1.25 s current ramp to delay the start of the data-integration period. Insufficient settling time at $t = 0.5$ s is clearly observed, and is attributed to the recovery of the feedback system from the large transient SQUID signal. The initial drift here is caused primarily by change in the current source output. Monitoring this current level during the CCC measurement was not possible due to added noise. As shown by (4), a closer match of R_1/R_2 to the CCC winding ratio N_1/N_2 would reduce the dependence on the measurement current and also presumably reduce the transient SQUID error signal.

IV. 100 MΩ CCC Noise Performance

Fig. 4 shows the SQUID output flux-noise spectrum of the 100 MΩ system, with the 96.2 MΩ cryogenic resistance sample being compared to the QHR $i = 2$ ($R_\mathrm{H} = 12\,906.4035\ \Omega$) resistance step at a current I_0 of 73 μA, using the CCC bridge with SQUID feedback. The primary winding consists of 15 496 turns of 76 μm diameter phosphor-bronze wire and has a resistance of about 60 kΩ at 293 K and 47.949 kΩ ± 0.5 Ω at 4.2 K. The noise resonance at center frequency $f_0 \approx 2.7$ kHz (see Fig. 4) reflects the large number of turns and high-inductance L in the resistive primary winding, with the noise resonance being set up by the main winding inductance and shunt capacitance. The phosphor-bronze wire resistance value was chosen to be approximately $R = 4\pi L f_0$ to strongly damp the noise resonance. A much sharper resonance at a center frequency of 1.75 kHz was observed in a 30 000 turn CCC [7] without this damping mechanism. Internal copper shields were not found to be effective at damping the resonance at low temperature in that work.

The 100 MΩ CCC detector is a commercial dc-SQUID coupled to the CCC by a flux-transformer, with a sensitivity level near 3.75 μA-turn/Φ_0 which implies a current sensitivity of 242 pA/Φ_0 for the primary winding. For comparison, the flux noise spectrum shown in Fig. 5 is typical for another two-terminal CCC with a superconducting 1937-turn primary winding and a similar 3.83 μA-turn/Φ_0 sensitivity. This CCC, as described in [3], is used to measure resistance ratios between the QHR and room-temperature 1 MΩ standards. The noise at low frequencies in Fig. 5 is due primarily to Johnson current noise in the 1 MΩ room-temperature resistor. The noise resonance amplitude generated by the superconducting winding at a center frequency $f_0 \approx 20$ kHz is larger than that observed in Fig. 4 for the 15 496 turn resistive winding. Normally, one would expect greater resonant noise amplitude for the larger winding if no damping was present since the SQUID gain increases at lower frequency. The effectiveness of resistive damping also is shown by the larger relative width of the resonance in Fig. 4.

The average flux noise level shown in Fig. 4 between 0.1 Hz and 25 Hz is approximately 44 $\mu\Phi_0/\mathrm{Hz}^{1/2}$, and this corresponds to a relative noise level of $1.13 \times 10^{-6}/\mathrm{Hz}^{1/2}$ at $I_0 = 73\ \mu$A. Calculations show this is in good agreement with the relative standard deviation of CCC resistance ratio data taken under similar conditions. The equivalent CCC current noise in the primary winding is 10.7 fA/Hz$^{1/2}$. Fundamental sources of noise include that of the SQUID, which averages about 5 $\mu\Phi_0/\mathrm{Hz}^{1/2}$, and the Johnson noise in the cryogenic resistor, contributing 6.1 $\mu\Phi_0/\mathrm{Hz}^{1/2}$. These combine for a limiting flux noise contribution of 8 $\mu\Phi_0/\mathrm{Hz}^{1/2}$, or a current noise level of 1.9 fA/Hz$^{1/2}$. Most noise between 0.1 Hz and 25 Hz is due to currents induced by the motion of QHR and CCC leads in stray magnetic fields. In particular, the CCC assembly is supported from the top of the cryostat by a 19-mm-diameter thin-wall tube and this creates a pendulum-mode mechanical oscillation near 3 Hz. Other high-sensitivity CCC devices with 30 000 or 20 000 turns [7], [8] have achieved flux noise levels as low as 27 $\mu\Phi_0/\mathrm{Hz}^{1/2}$ and CCC current noise levels of 2 fA/Hz$^{1/2}$ to 4 fA/Hz$^{1/2}$ over the frequency range 0.1–10 Hz. Those CCC devices however were characterized under conditions that did not include direct connections from the CCC to the QHR standard in a separate cryostat. Broadband noise in the range from 10 Hz to 100 Hz is low in this system, although it is not optimized for vibration or magnetic shielding and minimal filtering is employed.

Two guarded primary-side leads were added in place of the cryogenic resistor so that the bridge could be used with room temperature 100 MΩ resistors. The standard deviation of ratios obtained over three days with room temperature wire-wound resistors gave a relative noise level of $1.92 \times 10^{-6}/\mathrm{Hz}^{1/2}$. This

corresponds to a flux noise of about 74 $\mu\Phi_0/\mathrm{Hz}^{1/2}$. For this CCC, the Johnson noise component for a room temperature 100 MΩ resistor contributes 53 $\mu\Phi_0/\mathrm{Hz}^{1/2}$, or more than half of the total flux noise.

V. Comparison to Hamon Scaling Methods

Recently, we have used the 1 MΩ and 100 MΩ CCC systems described in the last section in comparisons with Hamon scaling networks [9] made up of 10 × 10 MΩ wire-wound resistors. These measurements of the 1 MΩ and 100 MΩ resistor configurations typically agree to within the combined relative uncertainty of 2.5×10^{-7} assigned for these CCC comparisons. It is very important to account for temperature dependence, voltage dependence, leakage, and settling effects in high-resistance comparisons because these effects are possibly the dominant sources of uncertainty. Thus, for most applications the Hamon scaling method is quite adequate for maintaining high resistance standards at the 100 MΩ level and above, and in this report serves as a test of the CCC scaling accuracy. The two-terminal CCC bridge has a relative uncertainty below 3×10^{-8} at the 1 MΩ level and compares favorably at that level with a similar-level four-terminal CCC method [10].

All Hamon devices were used with a guard voltage derived from the CCC current source output using a buffer amplifier. As shown in Fig. 2, the CCC windings are near ground potential. Due to the voltage across the resistive winding of the 100 MΩ CCC, its equivalent parallel leakage resistance must be of order 5×10^{12} Ω to produce less than 1×10^{-8} relative error. This level of insulation resistance readily can be obtained in cryogenic windings. This 15 496 turn winding was made up of two sections of 7748 turns. These two windings were tested in series-opposition to determine the winding-number accuracy and flux-cancellation error. Likewise, superconducting windings consisting of a few turns were tested in series-opposition. No flux-cancellation error was observed at a relative level below 1×10^{-8}.

VI. Conclusion

Two-terminal CCC resistance bridges have been used for comparisons of the QHR standard directly against resistance standards near 100 MΩ. The bridge was constructed with a primary winding resistance of order 50 kΩ. The internal resistance is effective at damping the noise resonance produced by the high-sensitivity 15 496-turn winding in this CCC. Similar damping should occur in larger windings where the resistance-to-inductance ratio is roughly the same, and should improve the performance of CCC bridges for ultra-sensitive current measurements.

To attain the highest accuracy, the CCC winding number ratio N_1/N_2 should be selected to match the resistance ratio R_1/R_2 including the winding resistance. Adding or subtracting windings in the primary arm might be simpler than trimming the resistance value of cryogenic resistors used in SET current measurements. This bridge operates within a factor of two of the Johnson noise level for room-temperature resistors and benefits from the reduced Johnson noise in cryogenic 100 MΩ resistors. The cryogenic resistance alloy should have as small a temperature coefficient of resistance as possible to minimize the long-term drift in its resistance value at low temperature. Thin-film cryogenic resistors are superior to conventional room-temperature 100 MΩ resistors by having lower inductance and capacitance and reduced dielectric effects, thus allowing faster current reversals. This should make it possible to reverse the current at a rate of 1 Hz or higher and to reduce the substantial effect of the $1/f$ SQUID noise component.

References

[1] D. B. Sullivan and R. F. Dziuba, "A low-temperature direct-current comparator bridge," *IEEE Trans. Instrum. Meas.*, vol. IM-23, pp. 256–260, 1974.

[2] I. K. Harvey, "Cryogenic ac Josephson effect emf standard using a superconducting current comparator," *Metrologia*, vol. 12, pp. 47–54, 1976.

[3] R. E. Elmquist, N. M. Zimmerman, and W. H. Huber, "Using a high-value resistor in triangle comparisons of electrical standards," *IEEE Trans. Instrum. Meas.*, vol. 52, no. 2, pp. 590–593, Apr. 2003.

[4] L. C. A. Henderson, "A new technique for the automatic measurement of high-value resistors," *J. Phys. E, Sci. Instrum.*, vol. 20, pp. 492–495, 1987.

[5] J. Kohlmann, P. Gutmann, and J. Niemeyer, "Ratio standard for dc resistance using a Josephson potentiometer," *IEEE Trans. Instrum. Meas.*, vol. 42, no. 2, pp. 255–257, Apr. 1993.

[6] F. Delahaye, "Series and parallel connection of multiterminal quantum Hall effect devices," *J. Appl. Phys.*, vol. 73, pp. 7915–7920, 1993.

[7] G. Rietveld, E. Bartolomé, J. Sesé, P. de la Court, J. Flokstra, C. Rillo, and A. Camón, "1:30 000 cryogenic current comparator with optimum SQUID readout," *IEEE Trans. Instrum. Meas.*, vol. 52, no. 2, pp. 621–625, Apr. 2003.

[8] N. Felton, L. Devoille, F. Piquemal, S. V. Lotkhov, and A. B. Zorin, "Progress in measurements of a single-electron pump by means of a CCC," *IEEE Trans. Instrum. Meas.*, vol. 52, no. 2, pp. 599–603, Apr. 2003.

[9] B. V. Hamon, "A 1–100 Ω build-up resistor for the calibration of standard resistors," *J. Sci. Instrum.*, vol. 31, pp. 450–453, 1954.

[10] E. Pesel, B. Schumacher, and P. Warnecke, "Resistance scaling up to 1 MΩ at PTB with a cryogenic current comparator," *IEEE Trans. Instrum. Meas.*, vol. 44, no. 2, pp. 273–275, Apr. 1995.